International Tables for X-ray Crystallography (1962). Vol. III, pp. 202–203. Birmingham: Kynoch Press.

IVANOV, V. T., KOGAN, G. A., TULCHINSKY, V. M., MIROSHNIKOV, A. V., MIKHALYOVA, I. I., EVSTRATOV, A. V., ZENKIN, A. A., KOSTESKY, P. V. & OVCHINNIKOV, YU. A. (1973). *FEBS Lett.* **30**, 199–204.

JOHNSON, C. K. (1965). *ORTEP*. Oak Ridge National Laboratory Report ORNL-3794.

NAWATA, Y. (1976). Unpublished work.

PAULING, L. (1960). *The Nature of the Chemical Bond*, 3rd ed. Ithaca: Cornell Univ. Press.

PIODA, L. A. R., WACHTER, H. A., DOHNER, R. E. & SIMON, W. (1967). *Helv. Chim. Acta*, **50**, 1373–1376.

PRESTEGARD, J. H & CHAN, S. I. (1970). *J. Amer. Chem. Soc.* **92**, 4440–4446.

SAKAMAKI, T., IITAKA, Y. & NAWATA, Y. (1976). *Acta Cryst.* B**32**, 768–774.

STEWART, R. F., DAVIDSON, E. R. & SIMPSON, W. T. (1965). *J. Chem. Phys.* **42**, 3175–3187.

UENO, M., KYOGOKU, Y. & NAWATA, Y. (1975). The 2nd Symposium on Molecular Structure of Biologically Related Substances, Tokyo, Japan.

Acta Cryst. (1977). B**33**, 59–69

X-ray Determination of the Electron Distribution in Crystals of $[Co(NH_3)_6][Cr(CN)_6]$ at 80 K

BY MIYUKI IWATA

The Institute for Solid State Physics, The University of Tokyo, Roppongi-7, Minato-ku, Tokyo 106, *Japan* and Chemistry Department, State University of New York at Buffalo, Buffalo, New York* 14214, *USA*

(*Received* 13 *May* 1976; *accepted* 15 *June* 1976)

X-ray diffraction data for a hexaamminecobalt(III) hexacyanochromate(III) single crystal were collected at 80 K. The crystal is isomorphous with $[Co(NH_3)_6][Co(CN)_6]$: space group $R\bar{3}$; $a_r = 7{\cdot}372$ (4) Å, $\alpha = 97{\cdot}93$ (3)°; $Z = 1$. The atom valence-scattering factors were refined to determine the electron populations and atomic parameters. The aspherical charge refinement shows that the valence-electron distributions of Co and Cr atoms outside the Ar core are related to the trigonal distortion of the complex ions. It also elucidates the difference between the bonding character of the metal–CN and metal–NH_3 bonds. The charges on Co and Cr are found to be largely neutralized. In addition, the net charges on an NH_3 molecule and a CN group are determined to be about +0·5 and −0·7 e respectively. Consequently, in agreement with the traditional chemical picture, $[Co(NH_3)_6]$ and $[Cr(CN)_6]$ have charges of +3 and −3 e respectively. The same conclusion is drawn from a similar analysis of the room-temperature data for a $[Co(NH_3)_6][Co(CN)_6]$ crystal; the charge on NH_3 is again +0·5, but on a CN group in $[Co(CN)_6]^{3-}$ the charge is −0·3 e.

Introduction

In recent years a number of molecular crystals, as well as simple crystals of high symmetry such as NaCl and diamond, have been investigated to determine electron distributions in solids by means of X-ray diffraction and/or neutron diffraction (Coppens, 1975). In many of their residual density maps, excess electrons are clearly observed in bond and lone-pair regions.

As for metallo-organic crystals, $[Co(NH_3)_6][Co(CN)_6]$ (hereafter abbreviated as [Co][Co]) was the first to be studied (Iwata & Saito, 1973). In the final residual density maps of this complex, an aspherical charge distribution around transition-metal atoms was found. In addition, excess electrons were observed in metal–ligand and C–N bond regions. Since then, several types of metal complexes have been examined in order to observe the aspherical distribution of electrons by difference syntheses (for example, γ-Ni_2SiO_4: Marumo, Isobe, Saito, Yagi & Akimoto, 1974; γ-Fe_2SiO_4: Marumo & Isobe, 1974; Marumo & Saito, 1974; γ-Co_2SiO_4: Marumo, Isobe & Akimoto, 1975; TiO_2: Shintani, Sato & Saito, 1975; an Rh complex: Miyamae, Sato & Saito, unpublished; a low-symmetry Co complex: Maslen, Ridout & White, 1975; a Ti complex: Manohar & Schwarzenbach, 1974). The direct observation of asphericity in electron distributions in metal complexes enables us to understand the physical and chemical nature of metal–ligand bonds, and of transition-metal complexes themselves.

Although the X-ray diffraction study of the title compound $[Co(NH_3)_6][Cr(CN)_6]$ (hereafter abbreviated as [Co][Cr]) was previously carried out at room

* Address for correspondence.

temperature (Iwata & Saito, unpublished), more accurate data are needed to demonstrate the electron redistributions caused by metal–ligand coordination. In the present study, the data were collected at 80 K to improve the accuracy.

Experimental

Crystals of [Co][Cr] were grown by a diffusion method from aqueous solutions of $[Co(NH_3)_6]Br_3$ and $K_3[Cr(CN)_6]$. They are orange-red hexagonal prisms. A crystal specimen ($1{\cdot}58 \times 10^{-2}$ mm^3 in volume) was sealed in a thin-walled glass capillary and mounted on a Picker FACS-1 diffractometer at Buffalo. The crystal was cooled by a conduction-type cryostat, developed by Coppens *et al.* (1974), to 80 ± 1 K with liquid nitrogen. Intensity data were collected with Mo $K\alpha$ radiation. Experiments at 80 K were performed twice: the second data collection (II) was made for the same crystal specimen eight months after the first (I) was completed. A θ–2θ step scan was employed; the scanning range was the calculated α_1–α_2 separation plus 1·5° (2·3°) for $2\theta \leq 45°$ ($2\theta \geq 45°$). Some other experimental conditions are summarized in Table 1. The eighteen extra standard reflexions were selected from each region of $\sin\theta/\lambda$ and F^2 in order to check the intensity variations more extensively.

All 21 standard reflexions remained stable within 2% in data collection I, while in experiment II the intensities of these reflexions began to drop, up to 10% at most, after the X-ray exposure for 1 week, because of radiation damage. The intensity drop was corrected as a function of exposure time and $\sin\theta/\lambda$, which was determined with about 500 duplicated reflexions observed both at the earlier and at the later stages of experiment II. The intensity drop was independent of the intensity itself.

A total of 9760 reflexions were recorded and processed by the programs *PROFILE* (calculation of integrated intensities by determining the background region of each reflexion profile by a computer analysis; Blessing, Coppens & Becker, 1974), *DATAPP* (absorption correction by numerical Gaussian integration; Coppens, Leiserowitz & Rabinovich, 1965; and scaling, including the correction for intensity drop by the radiation damage), and *DSORTH* (averaging symmetry-related reflexions, adopting certain criteria to discard unreliable reflexions from averaging).

Among the data of experiment I, the agreement between symmetry-related reflexions, $R(F^2)$, after correction for absorption, was good enough to be considered within the statistical errors (less than 2·3% for the 993 strongest reflexions). The agreement between the data of experiments I and II, after averaging symmetry-related reflexions, was 2·3% for 336 reflexions in the $2\theta \leq 45°$ region, which ensures that data II would be good enough for further analysis. Data I and II were finally combined and averaged to yield 2156 independent reflexions, of which 90 had negative values of F_o^2 and were rejected from the subsequent analyses.

The standard deviation of each reflexion was estimated from a comparison of the agreement between symmetry-related reflexions, in addition to the statistical counting errors:

$$[\sigma(I')]^2 = I + B + [0{\cdot}02I']^2 + [0{\cdot}015(I_{\text{corr.}} - I')]^2, \quad (1)$$

where I, B, and I' are the total observed intensity, the background intensity, and the net integrated intensity ($I' = I - B$) respectively, and $I_{\text{corr.}}$ is the integrated intensity after absorption correction.

The room-temperature data were collected on a Rigaku four-circle diffractometer at Hokkaido University. Some experimental conditions are listed in Table 1; these are similar to those described for the 'data set 1' of [Co][Co] in a previous paper (Iwata & Saito, 1973).

Lattice constants were determined from 30 automatically centred reflexions ($42 \leq 2\theta \leq 51°$) at 80 K

Table 1. *Experimental conditions for the two sets of data collection at* 80 *and* 298 K

	Experiment I at 80 K	Experiment II at 80 K	Experiment at 298 K
Crystal size	Hexagonal prism, 10 faces, vol. $= 1{\cdot}58 \times 10^{-2}$ mm^3		Cylinder, $r = 0{\cdot}105$, $l = 0{\cdot}2$ mm, vol. $= 6{\cdot}9 \times 10^{-3}$ mm^3
Radiation	Mo $K\alpha$	Mo $K\alpha$	Mo $K\alpha$
Scan method	θ–2θ step scan (every 1 s at each step)	0·03° in 2θ,	θ–2θ continuous scan (1° min^{-1} in 2θ, 15 s at each background)
$2\theta_{\text{max.}}$	45°	100°	120°
Monochromator	β-Filter (Zr)	β-Filter (Nb)	LiF(200)
Rotation axis of the crystal	Nearly parallel to $[111]_{\text{rhomb.}}$	Nearly parallel to $[11\bar{2}]_{\text{rhomb.}}$	Nearly parallel to $[111]_{\text{rhomb.}}$
Take-off angle	2·5°	3·5°	6°
Number of symmetry-related reflexions covered	6	3 or 2	1 to 3
Standard reflexion/interval	Ordinary 3/50 Extra 18/250	Ordinary 2/50 Extra 18/600	Ordinary 2/50
Total reflexions measured	2390	7370	2680
Independent reflexions ($F^2 \geq 0$)	336	2156	1815

and from 32 reflexions ($43 \leq 2\theta \leq 54°$) at 298 K, both with Mo $K\alpha$ radiation.

Crystallographic data are compared in Table 2. The space group was determined as for [Co][Co] and conforms to $R\bar{3}$. No structural change was found on cooling.

The computations were carried out on four computers: the CDC 6400 at the State University of New York at Buffalo, the IBM 370-195 at Argonne National Laboratory, the HITAC 8900 at the University of Tokyo, and the FACOM 230-48 at the Institute for Solid State Physics. The first was used for data processing of low-temperature data and preliminary refinements, and the other three were for the calculations of further refinements, difference Fourier syntheses, functional errors, *etc.* The last was also used for the refinement of the room-temperature data.

Refinement

In structural refinement, the quantity $\Delta = \Sigma w(F_o^2 - k^2F_c^2)^2$ was minimized. The weight w was determined as $w = 1/(\mathrm{Lp}A\sigma^2)$, where σ^2 is defined by equation (1), and Lp and A are Lorentz–polarization and absorption factors respectively. The starting parameters were those of the isomorphous [Co][Co] (Iwata & Saito, 1973). The valence-electron populations and valence-form factors [defined by $f(s/\kappa)$, instead of $f(s)$, where $s = \sin\theta/\lambda$, and κ was allowed to vary], as well as the positional and thermal parameters, a scale factor, and an extinction parameter, were refined by the least-squares program *RADIEL* (Becker, Yang & Coppens, unpublished) which is a modified version of *LINUS* (Coppens & Hamilton, 1970). By definition, the value of the parameter κ, *i.e.* less than or greater than 1·0, corresponds to an expansion or contraction of the atomic charge cloud relative to the reference state. The net charge in the crystal was constrained to be zero.

Two initial sets of atomic form factors for metals were tried. In set A, the Ar core was taken for the core electrons and $4s^2 + 3d^n$ [$n = 7$ (4) for Co(Cr)] for the valence electrons of the metals. The atomic form-factor table, which was calculated by Fukamachi (1971) from Hartree–Fock wave functions given by Clementi, was used. In set B, form factors for trivalent ions (M^{3+}) were taken for metal-core factors, and $f_{M^0} - f_{M^{3+}}$ for valence factors. *International Tables for X-ray Crystallography* (1974) was used in this case. In both sets A and B, the He core was considered to be the core for the electrons of the C and N atoms (from Fukamachi's table) and the hydrogen 1s electron was treated as a valence electron (*International Tables for X-ray Crystallography*, 1974). The anomalous dispersion terms for Co and Cr were taken from *International Tables for X-ray Crystallography* (1962).

When a pair of parameters was strongly correlated (correlation coefficient ≥ 0.8), they were refined alternately (not simultaneously) until they converged to their self-consistent values. The largest correlation (0·9) was found between the H temperature factor and the H κ.

It is necessary to refine κ and population parameters *etc.* in a self-consistent way, since both the electron population parameters and atomic parameters depend on the atomic form factors employed. This is illustrated in Table 3 for the [Co][Co] crystal where the bond lengths obtained by the traditional refinement (Iwata & Saito, 1973) are compared with those from the κ refinement. After the κ refinement, the bond lengths other than N–H became closer to the more reasonable values obtained by the traditional method with high-2θ data alone. The shorter N–H distances were obtained when all data were used, both with and without the κ refinements.

Although the κ refinement based on high-2θ data alone was attempted, convergence was not reached because of a small contribution of the H form factor to the high-angle reflexions.

An isotropic extinction correction was made. The smallest extinction factor y ($= F_o^2/F_c^2$) was 0·85 for $(2\bar{3}2)_{\mathrm{hexag.}}$, which was 0·89 in the room-temperature case.

Table 2. *Crystal data for* $[Co(NH_3)_6][Cr(CN)_6]$

F.W. 369·3, $F(000) = 189$, space group $R\bar{3}$ ($[C_{3i}^2$, No. 148).

	80 K	298 K
μ(Mo $K\alpha$)(cm^{-1})	19·91	19·78
D_m(g cm^{-3})		1·57$_3$ (291 K)
D_c	1·580	1·565
Rhombohedral setting		
a_r(Å)	7·372 (4)	7·394 (2)
α(°)	97·93 (3)	97·85 (2)
V(Å^3)	387·9 (5)	391·7 (2)
Z	1	1
Hexagonal setting		
a(Å)	11·122 (9)	11·148 (2)
c	10·864 (9)	10·919 (3)

Table 3. *Effects of* κ *refinement on bond lengths* (Å) *for* $[Co(NH_3)_6][Co(CN)_6]$

	κ all data	No κ all data*	No κ sin $\theta/\lambda > 0.6$*
Co–C	1·894 (1) Å	1·900 (1) Å	1·894 (1) Å
Co–N	1·973 (1)	1·968 (1)	1·972 (1)
C–N	1·152 (1)	1·146 (1)	1·157 (2)
N–H$_{av.}$	0·865 (2)	0·877 (10)	0·963 (55)

Details of the effects of κ refinement on the other parameters for [Co][Co] are available on request.

* Iwata & Saito (1973).

The final discrepancy indices are:

$R(F) = \Sigma|F_o - kF_c|/\Sigma|F_o| = 0.028$,
$R_w(F) = [\Sigma w(F_o - kF_c)^2/\Sigma wF_o^2]^{1/2} = 0.025$,
$R(F^2) = \Sigma|F_o^2 - k^2F_c^2|/\Sigma F_o^2 = 0.034$, and
$R_w(F^2) = [\Sigma w(F_o^2 - k^2F_c^2)^2/\Sigma wF_o^4]^{1/2} = 0.049$.

The refinement procedure, by *LINUS*, for the room-temperature data was similar to those described for 'data set 1' in a previous paper on [Co][Co] (Iwata & Saito, 1973). Neither higher-angle refinement nor κ refinement was performed since the data were not sufficiently accurate. The refinement was based on F and the final $R(F)$ and $R_w(F)$ were 0.048 and 0.039 respectively.*

Results and discussion

Crystal and molecular structure

The crystal consists of $[Co(NH_3)_6]^{3+}$ and $[Cr(CN)_6]^{3-}$ ions which are arranged in a rhombohedral cell in much the same way as those in the CsCl-type crystal. This is illustrated in Table 4. Of the eight surrounding counter ions, six are connected to the central ion by hydrogen bonds (dotted lines).

* A list of structure factors has been deposited with the British Library Lending Division as Supplementary Publication No. SUP 32018 (47 pp.). Copies may be obtained through The Executive Secretary, International Union of Crystallography, 13 White Friars, Chester CH1 1NZ, England.

Table 5 shows the final atomic parameters at the two temperatures. All the parameters are based on the hexagonal setting for the convenience of comparison with the previous results. The atomic parameters at 80 K are independent of the choice of the assumed form factors A or B, except for the temperature factors of Co. Table 6 lists the molecular dimensions calculated from these parameters. All values are corrected for thermal motion (Cruickshank, 1956*a*). The room-temperature values are from the traditional refinement adopting the full data. As discussed above (Table 3), this causes inaccuracies in the final parameters at 298 K and is partly the reason why the values at the two temperatures are in poor agreement, even after thermal-vibration corrections (Table 6). Insufficient correction for thermal motion, as well as the inaccuracy of the room-temperature data, is also responsible for the discrepancy between the results at the two temperatures (especially for the C—N bond length).

The largest difference between parameters at the two temperatures appears in the hydrogen-bonding modes: on cooling to 80 K, the N···N and N···H distances contract by about 0.03 and 0.06 Å respectively, and the NH···N angle increases by about 3° from the room-temperature values. Although these differences result partly from the errors mentioned above, they may also be a consequence of the real temperature effects which cause the contraction of the lattice at low temperature. In Table 4, it is shown that the distortion of the lattice

Table 4. *Distortions of the crystal lattice and geometries of the complex ions from cubic symmetry*

The columns (*a*) and (*c*) are based on the κ refinement, and are averaged values of the results evaluated by the initial form-factor sets A and B; (*b*) is based on a traditional refinement.

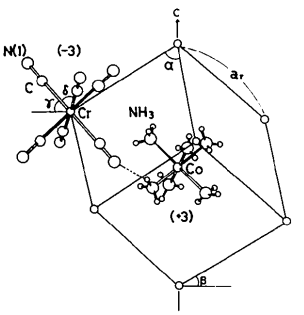

	(*a*) [Co][Cr], 80 K	(*b*) [Co] [Cr], 298 K	(*c*) [Co] [Co], 298 K	(*d*) Regular cube or O_h coordination
Unit-cell lattice				
a/c	1.024 (1)	1.021 (1)	1.014 (1)	0.8165
α	97.93 (3)°	97.85 (2)°	97.65 (2)°	90°
β	29.42 (1)	29.50 (1)	29.65 (2)	35.31
Complex ions				
γ(M–L) L = CN	35.15 (3)	35.62 (8)	35.12 (3)	35.31
L = NH_3	35.62 (3)	35.39 (10)	35.36 (3)	
δ(LML') L = CN	90.16 (4)	89.49 (13)	90.22 (6)	90
L = NH_3	89.50 (3)	89.85 (13)	89.87 (6)	

from cubic symmetry is the largest in [Co][Cr] at 80 K.

Another difference in the geometries at the two temperatures is found in the angle δ(LML'), the bond angle between the ligands L and L' related by the threefold axis. On cooling the crystal, the angle δ changes in opposite directions in $[Cr(CN)_6]^{3-}$ and $[Co(NH_3)_6]^{3+}$ (Tables 4 and 6); the $[Cr(CN)_6]^{3-}$ ion is compressed along the threefold axis, while $[Co(NH_3)_6]^{3+}$ is elongated in this direction at 80 K. The electron populations under such distortion will be discussed below. The geometry of the $[Co(NH_3)_6]^{3+}$ ion is very similar in [Co][Co] and [Co][Cr] at room temperature (Table 4).

Thermal motion

The r.m.s. amplitudes of the atoms in the crystals are given in Table 7. The average values of those determined with form-factor sets *A* and *B* are given for 80 K; the differences between these two sets of values are within their standard deviations except for Co. The vibrational amplitudes decrease about 40% on cooling to 80 K. The fourth and seventh columns in Table 8 give Δ (the definition is given in the table), which is a measure of rigidity of the complex ions. It also decreases by an order of magnitude on cooling to 80 K.

Scale factor, extinction, and κ parameters

The effects of the initial form factors on the scale factors, extinction factors, and κ's, are examined for both [Co][Cr] (80 K) and [Co][Co] (298 K) in Table 9. The effect on the scale factors is not significant (about 1% for both crystals). The scale factor for

Table 6. *Interatomic distances* (Å) *and bond angles* (°) *in* $[Co(NH_3)_6][Cr(CN)_6]$

All values are corrected for thermal vibrations.
Symmetry-code superscript (i) $\frac{2}{3} - y, \frac{1}{3} + x - y, \frac{1}{3} + z$.

	80 K *f* set *A*	80 K *f* set *B*	298 K Traditional refinement
Cr–C	2·071 (1)	2·071 (1)	2·080 (3)
Co–N(2)	1·979 (1)	1·980 (1)	1·970 (3)
C–N(1)	1·156 (1)	1·157 (1)	1·137 (3)
N(2)–H(1)	0·859 (11)	0·853 (12)	0·845 (62)
N(2)–H(2)	0·864 (9)	0·860 (10)	0·816 (46)
N(3)–H(3)	0·856 (8)	0·859 (9)	0·833 (40)
C–Cr–C*	90·16 (4)	90·15 (4)	89·49 (13)
N(2)–Co–N(2)*	89·47 (3)	89·54 (3)	89·85 (13)
Cr–C–N(1)	177·50 (4)	177·50 (5)	176·88 (14)
Co–N(2)–H(1)	113·8 (7)	113·8 (8)	109·6 (33)
Co–N(2)–H(2)	113·3 (6)	113·2 (7)	112·9 (30)
Co–N(2)–H(3)	111·7 (6)	112·0 (6)	111·1 (13)
H(1)–N(2)–H(2)	104·4 (10)	104·8 (10)	110·8 (40)
H(1)–N(2)–H(3)	104·6 (9)	104·5 (10)	104·9 (39)
H(2)–N(2)–H(3)	108·5 (8)	108·0 (9)	107·1 (40)
Hydrogen bond: N(2)–H(3)···N(1)^{i}			
N(2)···N(1)^{i}	2·978 (2)	2·975 (2)	3·006 (4)
H(3)···N(1)^{i}	2·138 (9)	2·132 (10)	2·197 (71)
N(2)–H(3)···N(1)^{i}	166·8 (8)	167·1 (9)	163·8 (32)

* The angle between atoms related by a threefold axis.

Table 5. *Final atomic coordinates (fractional) and thermal parameters with their e.s.d.'s (hexagonal setting)* ($\times 10^5$)

Anisotropic thermal parameters are of the form $\exp[-(h^2\beta_{11} + k^2\beta_{22} + l^2\beta_{33} + 2hk\beta_{12} + 2hl\beta_{13} + 2kl\beta_{23})]$, except for H atoms, which have the isotropic form $\exp(-B\sin^2\theta/\lambda^2)$. The '(*a*)' rows give the values at 80 K, with the form-factor set *A*; '(*b*)' at 80 K, with the form-factor set *B*, both with *RADIEL*; and '(*c*)' at 298 K by a traditional refinement with *LINUS*.

	x	*y*	*z*	β_{11}	β_{22}	β_{33}	β_{12}	β_{13}	β_{23}
Cr (*a*)	0	0	0	143 (1)	143 (1)	104 (1)	71 (1)	0	0
(*b*)	0	0	0	139 (1)	139 (1)	102 (1)	69 (1)	0	0
(*c*)	0	0	0	393 (5)	393 (5)	298 (6)	197 (3)	0	0
Co (*a*)	0	0	50000	113 (1)	113 (1)	98 (1)	56 (1)	0	0
(*b*)	0	0	50000	121 (1)	121 (1)	105 (1)	60 (1)	0	0
(*c*)	0	0	50000	329 (4)	329 (4)	261 (5)	165 (2)	0	0
N(1) (*a*)	21536 (5)	25097 (5)	17358 (5)	434 (6)	230 (5)	276 (5)	136 (5)	−112 (4)	−52 (4)
(*b*)	21536 (6)	25099 (5)	17361 (5)	439 (6)	234 (5)	278 (5)	138 (5)	−113 (5)	−53 (4)
(*c*)	20843 (23)	24925 (20)	17486 (21)	1110 (26)	569 (17)	707 (17)	302 (18)	−279 (17)	−138 (14)
C (*a*)	14074 (6)	16143 (6)	10967 (5)	254 (5)	209 (4)	173 (3)	116 (4)	−10 (3)	9 (3)
(*b*)	14071 (6)	16140 (6)	10967 (5)	256 (5)	211 (4)	173 (4)	118 (4)	−9 (3)	10 (3)
(*c*)	13784 (23)	16192 (24)	11074 (21)	612 (20)	465 (17)	415 (15)	242 (16)	−54 (14)	−10 (13)
N(2) (*a*)	12713 (4)	15706 (5)	60602 (4)	181 (4)	167 (4)	153 (3)	62 (3)	−15 (2)	−23 (2)
(*b*)	12714 (5)	15708 (5)	60602 (4)	183 (4)	170 (4)	156 (3)	64 (3)	−15 (2)	−23 (2)
(*c*)	12496 (21)	15693 (22)	60418 (19)	486 (16)	469 (16)	390 (13)	169 (13)	−42 (12)	−64 (12)

	x	*y*	*z*	*B*		*x*	*y*	*z*	*B*
H(1) (*a*)	9852 (83)	31416 (81)	62161 (80)	4·02 (16)	H(3) (*a*)	20641 (90)	20670 (91)	57204 (85)	4·01 (17)
(*b*)	9872 (86)	21419 (89)	62157 (81)	3·53 (24)	(*b*)	20686 (107)	20681 (100)	57228 (85)	3·50 (25)
(*c*)	9253 (468)	21007 (452)	61340 (385)	5·16 (112)	(*c*)	20096 (444)	20492 (424)	57041 (373)	4·24 (99)
H(2) (*a*)	13971 (79)	13144 (85)	67760 (79)	3·27 (16)					
(*b*)	14013 (80)	13152 (86)	67738 (92)	2·81 (24)					
(*c*)	13965 (408)	13279 (421)	67004 (391)	3·64 (89)					

[Co][Co] determined previously by the traditional method (Iwata & Saito, 1973) from the full data is 8·959 (5), which is not significantly different from the present result, but that from high-2θ data is larger by about 2% than the present values. It is generally found that the effect of the choice of the form factors (*A* or *B*) on a parameter is significant only when the parameter is strongly correlated with the other parameters. For example, since the scale factor and the extinction parameter in [Co][Co] (with form-factor set *A*), are correlated [the correlation coefficient (c.c.) is 0·7], the apparent effect of the form factor, both on the scale factor and on the extinction factor, is larger in [Co][Co] (298 K) than in [Co][Cr] (80 K) in which the c.c. is <0.5 for both sets *A* and *B*.

Fig. 1 shows the atomic form factors for (*a*) Cr and

Table 7. *R.m.s. amplitudes* ($\times 10^3$ Å) *of thermal motion along principal axes and their components* ($\times 10^4$) *along crystal axes*

	Principal axes, components along crystal axes*			R.m.s. amplitudes [Co][Cr]† 80 K	[Co][Cr] 298 K	[Co][Co]† 298 K
Cr/Co(1)	651	1026	0	82	136	122
	414	−618	0	82	136	122
	0	0	921	79	134	120
Co(2)	0	0	921	78	126	121
	888	910	0	74	125	118
	−512	527	0	74	125	118
N(1)	836	166	−481	161	259	232
	268	−431	676	120	197	182
	554	930	399	98	153	139
C	909	162	−335	111	179	161
	−501	−673	−681	103	154	147
	71	774	−522	96	148	136
N(2)	520	−483	237	103	171	160
	536	311	−787	99	160	153
	721	865	415	83	135	122
H(1)‡				219	256	248
H(2)‡				196	215	244
H(3)‡				218	232	236

* Values from [Co][Cr] (at 80 K, with form-factor set *A*) are listed, since the orientation of the thermal ellipsoids is essentially the same for all cases.

† Values from refinements based on form-factor sets *A* and *B* are averaged.

‡ Hydrogen atoms were assumed to move isotropically.

Table 9. *Effects of atomic form factors on various parameters*

	(*a*) [Co][Cr], 80 K *f* set *A*	(*b*) [Co][Cr], 80 K *f* set *B*	(*c*) [Co][Co], 298 K *f* set *A*	(*d*) [Co][Co], 298 K *f* set *B*
Scale factor	3·353 (3)	3·371 (4)	8·863 (8)	8·952 (5)
Extinction parameter	1·12 (12)	1·25 (14)	0·85 (5)	1·06 (4)
κ Cr/Co(1)	1·118 (20)	1·118 (31)	0·942 (7)	1·028 (12)
κ Co(2)	1·003 (12)	1·107 (29)	1·075 (9)	0·973 (13)
κ N(1)	0·922 (4)	0·923 (3)	0·982 (2)	0·996 (2)
κ C	1·044 (4)	1·022 (4)	1·087 (3)	1·064 (3)
κ N(2)	1·003 (4)	0·997 (3)	0·966 (3)	0·993 (2)
κ H	1·535 (65)	1·444 (49)	1·557 (25)	1·331 (15)

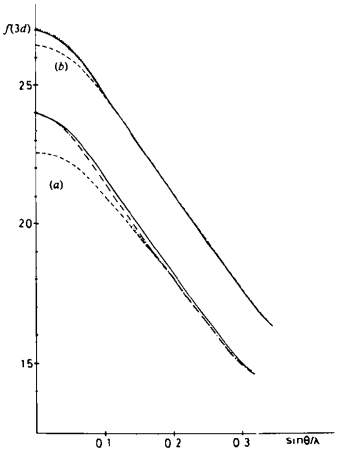

Fig. 1. Improvement of the form factors, $f(3d)$, by the κ and population refinement for (*a*) Cr and (*b*) Co in $[Co(NH_3)_6][Cr(CN)_6]$; the initial form factors: set *A* (— · —) and set *B* (——); factors modified by κ and populations: from set *A* (· · ·) and set *B* (– – –).

Table 8. *Rigidity of the complex ions*

Hydrogen atoms are eliminated from the summation and the rigid-body analysis. *T*: translational amplitudes; ω: rotational amplitudes (Cruickshank, 1965*b*); averaged values of the results with form factor sets *A* and *B* are given for 80 K.

	80 K			298 K		
	T	ω	Δ*	*T*	ω	Δ*
$[Cr(CN)_6]^{3-}$	0·088 Å	1·82°	0.55×10^{-2} Å^2	0·136 Å	3·04°	0.31×10^{-1} Å^2
	0·088	1·96		0·136	3·10	
	0·085	2·12		0·141	3·55	
$[Co(NH_3)_6]^{3-}$	0·076	1·79	0.70×10^{-4}	0·127	2·89	0.51×10^{-3}
	0·076	1·80		0·127	2·94	
	0·080	2·14		0·128	3·52	

* $\Delta = \sum_{\text{atom}} \sum_{ij} w(U_{ij}^{\text{obs.}} - U_{ij}^{\text{calc.}})^2$, w = atomic weight.

(*b*) Co, before and after the κ (Table 9) and population (Table 10) refinements, for both the initial form factors *A* and *B*. After the refinement, the modified form factors agree with each other at $\sin\theta/\lambda \geq 0{\cdot}15$, independent of the choice of the initial form factors. As for the lighter atoms, it is shown in Table 9 that the radial contraction ($\kappa > 1$) of electron distribution takes place for C and H atoms on forming chemical bonds, while for both the nitrogens of the cyano and ammonia groups, the radial expansion ($\kappa < 1$) occurs, in both [Co][Cr] and [Co][Co].* The same trend was also observed elsewhere (Griffin & Coppens, 1975).

In each crystal, the apparent effect of the initial form factors on a κ value is again large when the κ has a large correlation (c.c. $> 0{\cdot}7$) with the corresponding population parameter. Qualitatively speaking, however, the κ refinement gives consistent features for the radial distribution of electrons for all atoms, irrespective of the initial form factors.

Electron population

Table 10 shows the effective charges on atoms and groups of atoms, obtained by population refinement by *RADIEL*. The effect of atomic form factors is again large when a population parameter is strongly correlated with κ (c.c. $> 0{\cdot}73$). Thus, apart from quantitative details, the following general remarks can be drawn, independent of the initial form factors: (i) Both crystals consist of definite ionic species, $[Co(NH_3)_6]^{3+}$ and $[M(CN)_6]^{3-}$ [M = Cr or Co(1)]. (ii) The central metal atoms themselves are largely neutralized rather than +3 e (*cf.* Table 12). The results from direct integration of electron densities in a sphere of 1·08 Å [the minimum of radial electron distribution $4\pi r^2\rho(r)$ *versus* radius *r*] around the central metal atoms may be compared with those in Tables 10 and 12: namely, 23·0 for Cr and 26·0 for Co, *i.e.* both metals have a charge of +1 e at 80 K (the corresponding values at 298 K are 22·6 for Cr and 26·0 e for Co with $r = 1{\cdot}22$ Å, which is also determined as above). (iii) Consequently, the charge redistributions take place in the complex ions: CN is negatively charged (its negativity is larger in $[Cr(CN)_6]^{3-}$ than in $[Co(CN)_6]^{3-}$), the polarization is C^+–N^-, and N in $[Cr(CN)_6]^{3-}$ is again more negative than in $[Co(CN)_6]^{3-}$; NH_3 has a positive charge of about +0·5 e in both crystals; the hydrogens are positively charged and the values (about +0·2 e) roughly agree with other results (Coppens, Pautler & Griffin, 1971; Griffin & Coppens, 1975).

Residual electron density maps

Fig. 2(*a*) shows the $(F_o - F_c)$ synthesis on a plane passing through a Co–N bond and the threefold axis of the complex, with the atomic form-factor set *A*. The results with form-factor set *B* are similar. The four peaks around the Co atom are similar to those observed in [Co][Co] (Iwata & Saito, 1973) and appear at chemically equivalent positions. Of these peaks, two which lie on the threefold axis differ from the other two, both in peak heights and in peak positions (Table 11). The similar map on a section through a Cr–CN bond and the threefold axis is shown in Fig. 2(*b*). The four peaks near the Cr atom are here seen again (see Table 11). These peaks were supposed, in a previous paper (Iwata & Saito, 1973), to be due to the asphericity in 3*d* electron distributions. It is noted that their peak positions and peak heights are correlated with the trigonal distortions of the complex ions. In the $[Cr(CN)_6]^{3-}$ complex ion at 80 K, for example, the angle δ is greater than 90° (Table 4) and the two residual peaks on the threefold axis appear at a closer distance to Cr, with a larger peak height, than the other two; on the other hand, the opposite trend was observed in $[Co(NH_3)_6]^{3+}$, in the same crystal, where δ is significantly smaller than 90°. Although the distances from the metals are less accurate because of the limitation in

* The exception is found in Table 9, column (*a*) for N(2), where κ is slightly, but not significantly, larger than 1·0.

Table 10. *Electronic charges on atoms and groups*

	[Co][Cr], 80 K		[Co][Co], 298 K	
	f set *A*	*f* set *B*	*f* set *A*	*f* set *B*
Cr/Co(1)	+0·64 (9) e	+1·42 (9) e	−0·99 (8) e	−1·04 (7) e
Co(2)	−0·06 (8)	+0·52 (9)	+0·11 (8)	−0·71 (8)
N(1)	−0·83 (3)	−0·76 (3)	−0·54 (2)	−0·37 (2)
C	+0·18 (2)	−0·01 (2)	+0·22 (2)	+0·11 (2)
N(2)	−0·01 (4)	−0·05 (4)	−0·62 (4)	−0·16 (5)
H(1)	+0·14 (3)	+0·12 (3)	+0·35 (3)	+0·22 (3)
H(2)	+0·22 (2)	+0·20 (2)	+0·38 (3)	+0·25 (3)
H(3)	+0·20 (2)	+0·18 (2)	+0·36 (2)	+0·23 (3)
CN	−0·65 (4)	−0·77 (4)	−0·32 (3)	−0·26 (3)
NH_3	+0·55 (6)	+0·45 (6)	+0·47 (6)	+0·55 (7)
$[M(CN)_6]$*	−3·25 (13)	−3·22 (13)	−2·91 (11)	−2·60 (10)
$[Co(NH_3)_6]$	+3·25 (17)	+3·22 (17)	+2·93 (17)	+2·61 (19)

* M = Cr or Co(1) for hexacyanides.

Table 11. *Residual density peaks* (e Å^{-3}) *around metal atoms*

	[Co][Cr], 80 K		[Co][Co], 298 K	
	Peak height	Distance from metal	Peak height	Distance from metal
$[M^*(CN)_6]^{3-}$				
On threefold axis (a_g)	0·84	0·30 Å	0·76	0·39 Å
On $e_g(t_{2g})$†	0·67	0·57	0·59	0·49
$[Co(NH_3)_6]^{3+}$				
On threshold axis (a_g)	0·72	0·44	0·67	0·49
On $e_g(t_{2g})$†	1·02	0·53	0·50	0·51

* M = Cr or Co(1).

† The direction which is chemically equivalent to a_g (see Appendix).

resolution, such a correlation is also observed in the following examples: in the corresponding map of γ-Fe_2SiO_4 (Marumo & Isobe, 1974; Marumo & Saito, 1974); in [Co][Co] after refinement by *RADIEL* (Tables 4 and 11) (the exception for the peak heights in $[Co(NH_3)_6]^{3+}$ of this crystal may be caused by the small deviation of this ion from cubic symmetry, and by thermal smearing); and even in the less accurate maps of [Co][Cr] at room temperature (Fig. 3 and Table 4).

The bonding electrons are clearly seen in the Co–NH_3, Cr–C and C–N bonds. The last two peaks are elongated more than the first and may represent π-bonding features which were also observed in [Co][Co]. The cross-sections perpendicular to these bonds at the mid-bond peaks are shown in Fig. 4(*a*)–(*c*). The peaks in Fig. 4(*b*) and (*c*) are not as circular as in (*a*), probably reflecting the difference in bond character. Fig. 4(*d*) shows the section parallel to the plane of Fig. 4(*b*) and (*c*) and through Cr. The four peaks in this figure roughly correspond to those in Fig. 2(*b*), and their maxima are about 45° off those in Fig. 4(*b*) and (*c*), which has not yet been clearly interpreted.

The standard deviation of electron density is 0·06 e $Å^{-3}$ at general positions and 0·2 e $Å^{-3}$ at metal sites (Cruickshank & Rollett, 1953).

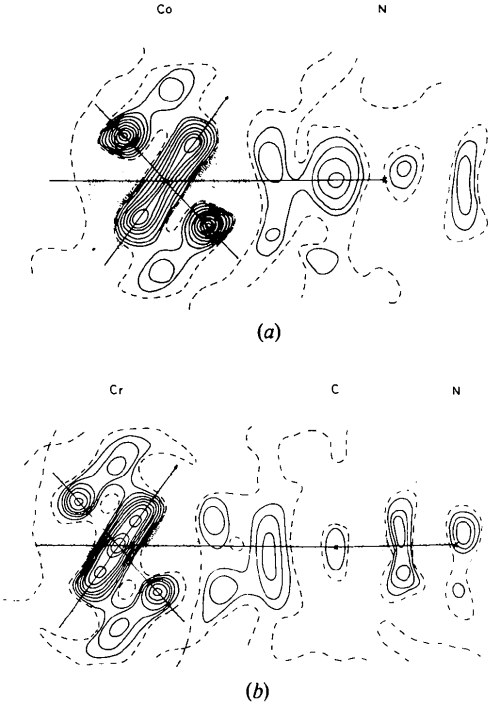

Fig. 2. $F_o - F_c$ map of $[Co(NH_3)_6][Cr(CN)_6]$ at 80 K after the κ refinement: (*a*) in a section through a Co–N bond and the threefold axis (▲); (*b*) in a section through a Cr–CN bond and the threefold axis. Contours are at 0·1 e $Å^{-3}$ intervals: negative contours (· · ·); zero contour (— · —). The crosses indicate the atom positions.

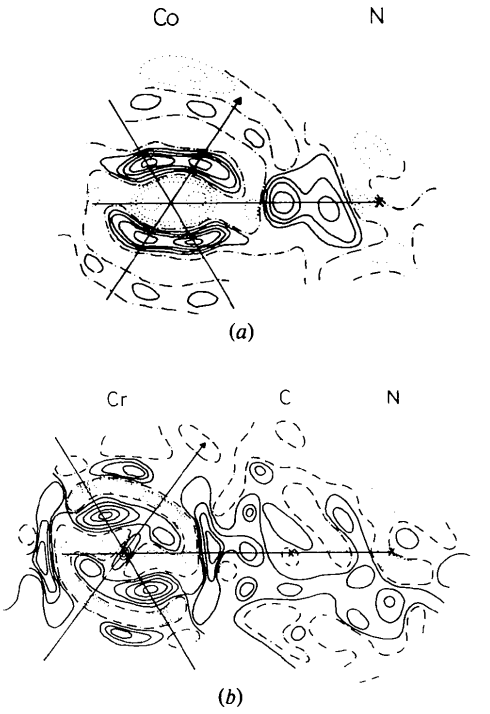

Fig. 3. $F_o - F_c$ map of [Co][Cr] at room temperature without the κ refinement: (*a*) the section through a Co–N bond and the threefold axis; (*b*) the section through a Cr–CN bond and the threefold axis. Contours are at 0·1 e $Å^{-3}$ intervals.

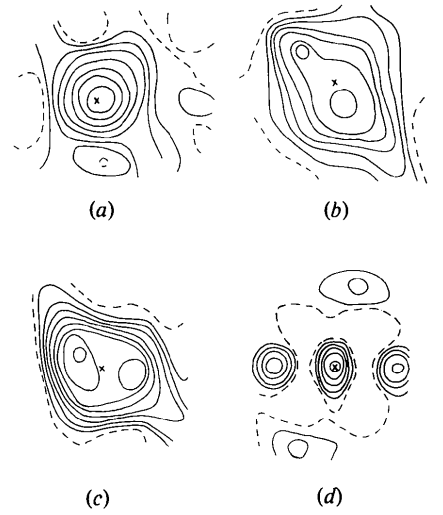

Fig. 4. $F_o - F_c$ maps of [Co][Cr] at 80 K after the κ refinement, on sections (*a*) perpendicular to a Co–N bond and through the mid-bond peak (0·46 Å from N) (the approximate radius of the circle, r [from the bond (X) to the zero contour], is about 0·5 Å); (*b*) perpendicular to a Cr–C bond and through the bond peak (0·62 Å from C, $r \sim 0.7$ Å); (*c*) perpendicular to a C–N bond and through the peak maximum (at the mid-point) of the bond ($r \sim 0.55$ Å); (*d*) perpendicular to a Cr–C bond and through a Cr atom site. Contours are at 0·05 e $Å^{-3}$ intervals for (*a*)–(*c*) and 0·2 e $Å^{-3}$ for (*d*).

Aspherical charge refinement

The aspherical charge refinement was carried out to examine the deformation of the electron distributions around metals. To perform the analysis the following assumptions were made: (i) The parameters of the metals are not correlated with those of lighter atoms {this is true for [Co][Co]; however, in [Co][Cr], the Cr population parameter is correlated with that of N(1) (c.c. = −0·61)}, then all the parameters of the lighter atoms and the temperature factors of metals are fixed at the values obtained by *RADIEL*, with the form-factor set *A*. (ii) The metal valence electrons outside the Ar core are all regarded as 3*d* electrons, and their form factors are expressed as a linear combination of scattering factors (f_j) of trigonally distorted 3*d* orbitals (j), each multiplied by the population parameter (n_j) which is to be determined by this analysis; ΔF was fitted as $\Delta F = \Sigma\, n_j f_j$ by the least-squares refinement (see Appendix), where $\Delta F = F_{obs.} - F$(light atoms)−F(metal cores).

In the present analysis, 195 and 375 reflexions with a large absolute value of ΔF were used for [Co][Cr] (80 K) and [Co][Co] (298 K) respectively. The 3*d* form factors for the a_g, $e_g(t_{2g})$ and $e_g(e_g)$* components under a trigonal field are given in the Appendix [equations (*A*3)–(*A*5)] in terms of the angular coordinates of the scattering vector of each reflexion and the $\langle j_n \rangle$'s, the expectation value of the nth Bessel function, which are tabulated in *International Tables for X-ray Crystallography* (1974). The $\langle j_n \rangle$'s for 3*d* electrons of neutral Co and Cr were used, since some population parameters with unreasonably negative values were obtained if $\langle j_n \rangle$'s for trivalent ions were used.

The aspherical population parameters thus obtained are given in Table 12. Although the standard deviations are large, because only a small number of reflexions were used at this stage where the lighter atoms are not taken into consideration, the following remarks may be made, from the results in Table 12, on the differences between NH_3 and CN, and between Co and Cr, and, in addition, on the temperature effects.

The dependence on the ligands and on the metals

It is notable that when the ligand is CN (shown in the upper part of Table 12), the electron population, $n[e_g(e_g)]$, in the $e_g(e_g)$ orbital, is smaller than that expected for the spherically symmetric distribution in the neutral atoms {$n^0[e_g(e_g)] = 2{\cdot}4$ [40%] and 3·6 [40%] for Cr^0 and Co^0 respectively}. On the other hand, when NH_3 is the ligand (shown in the lower part of Table 12), $n[e_g(e_g)]$ is found to be larger than that expected for Co^0.*

The ligand dependence of $n[e_g(t_{2g})]$, and of $n(t_{2g})$, the sum of $n(a_g)$ and $n[e_g(t_{2g})]$, in percentage, is opposite to that of $n[e_g(e_g)]$.* If the electron population is compared with $n^0(t_{2g})$ of trivalent ions in an O_h field, it is

* The parentages of an octahedral field are given in parentheses to differentiate the two types of e_g orbitals in a trigonal environment.

* See footnote to Table 12.

Table 12. *Valence electron population on metal atoms*

The number of electrons with their standard deviations are in parentheses, percentages in square brackets. The atoms in the upper part of the table are coordinated by $(CN)_6$, and those in the lower part, by $(NH_3)_6$. Values in the columns 'M⁰' are obtained by dividing the number of valence electrons (6 for Cr and 9 for Co) outside the Ar core in free metals into 1 : 2 : 2 (spherical).

		[Co][Cr], 80 K				[Co][Co], 298 K			
				Cr^0				Co^0	
Cr/Co(1)	a_g	0·97 (58) [17·7%]	3·32 [60·7%]	1·2 [20%]	3·6 [60%]	1·90 (31) [20·3%]	6·18* [65·9%]	1·8 [20%]	5·4 [60%]
	$e_g(t_{2g})$	2·35 (82) [43·0]		2·4 [40]		4·28 (47)* [45·6]		3·6 [40]	
	$e_g(e_g)$	2·15 (115) [39·3]		2·4 [40]		3·20 (63) [34·1]		3·6 [40]	
	Total	5·47 (153)		6·0		9·38 (84)		9·0	
	Charge	+0·53 e		0·0 e		−0·38 e		0·0 e	
				Co^0				Co^0	
Co(2)	a_g	1·34 (65) [15·0]	4·32 [48·3]	1·8 [20]	5·4 [60]	1·79 (30) [18·9]	5·03 [53·0]	1·8 [20]	5·4 [60]
	$e_g(t_{2g})$	2·98 (102) [33·3]		3·6 [40]		3·24 (47) [34·1]		3·6 [40]	
	$e_g(e_g)$	4·64 (147)* [51·8]		3·6 [40]		4·46 (63)* [47·0]		3·6 [40]	
	Total	8·96 (177)		9·0		9·49 (84)		9·0	
	Charge	+0·04 e		0·0 e		−0·49 e		0·0 e	

* The number of electrons in the t_{2g} or e_g orbitals is larger than 6 or 4 respectively, which may result from the assumption that all the electrons outside the Ar core are regarded as 3*d* electrons. The hybridization of 3*d* with 4*s* and 4*p* orbitals possibly plays a certain role.

also found that $n(t_{2g})$ is larger, in CN coordination, than that of Cr^{3+} or Co^{3+}, while it is smaller, in NH_3 coordination, than that expected for Co^{3+} [$n^0(t_{2g}) = 3{\cdot}0$ for Cr^{3+} and $6{\cdot}0$ for Co^{3+}].*

The order of all these population numbers is consistent with the order of the energy gaps $\Delta\epsilon = \epsilon(e_g) - \epsilon(t_{2g})$ between higher e_g and lower t_{2g} orbitals of the complex ions in an octahedral field {$\Delta\epsilon[Co(CN)_6] > \Delta\epsilon[Cr(CN)_6] > \Delta\epsilon[Co(NH_3)_6]$; Jørgensen, 1962}. Furthermore, since the $e_g(e_g)$ orbital has its maximum along the metal–ligand bond and it forms σ bonds with both the CN and NH_3 ligands, the larger $n[e_g(e_g)]$ may possibly be related to a greater σ character in the Co–NH_3 bond, compared with the M–CN bond. On the other hand, since a_g and $e_g(t_{2g})$ orbitals have π character and form π bonds with CN, $n(t_{2g})$ might also be related to the degree of π character in CN coordination, and to the difference in the charges of CN's in the two kinds of hexacyanides (Table 10).

$n(a_g)$ and the significance of the results

If the angle σ(LML′) is significantly smaller than 90°, it is expected that the population along the threefold axis [$n(a_g)$] would be smaller than that in a free atom. This seems to be the case, at least for $[Co(NH_3)_6]^{3+}$ at 80 K (Tables 4 and 12), and is consistent with the residual density maps [Fig. 2(a) and Table 11].

It is also noted that when the population parameters (n's) were treated as independent parameters, the approximate ratio of 1 : 2 : 2 was obtained for the n's of a_g, $e_g(t_{2g})$, and $e_g(e_g)$. These observations may support the positivity of the results of Table 12, although the present analysis contains many approximations and errors.

The author wishes to express her gratitude to Professor Y. Saito for his keen interest, continuous encouragement and helpful advice during the course of the work. She expresses her sincere thanks to Professor P. Coppens of State University of New York at Buffalo, for his hospitality, for making all the facilities and programs available to her, and for his helpful suggestions. Thanks are also due to Dr J. M. Williams of Argonne National Laboratory for the use of an IBM 370 under the auspices of the US Energy Research and Development Administration. She is much indebted to the members of Professor Coppens's group, particularly to Dr R. H. Blessing, for their kind help during the low-temperature experiment and data processing, and to Professor T. Mitsui for the use of the diffractometer at Hokkaido University (room-temperature experiment). That part of the work done at Buffalo was supported by National Science Foundation MPS 7102783A05, and at Tokyo by a Scientific Research Grant of the Ministry of Education, to both of which the author's thanks are due.

* See footnote to Table 12.

APPENDIX

For the analysis of the trigonal distortions of the electron distribution, the threefold axis of the crystal is taken as the z-(quantization) axis. In this coordinate system, the $3d$ orbitals of the central metals in a C_{3i} environment are given in terms of d_m ($m = \pm2, \pm1, 0$) as follows:

$$\begin{aligned} &a_g : d_0 \\ &e_g(t_{2g}) : \left.\begin{matrix} \sqrt{(2/3)}d_2 - \sqrt{(1/3)}d_{-1} \\ \sqrt{(2/3)}d_{-2} + \sqrt{(1/3)}d_1 \end{matrix}\right\} : t_{2g}[O_h] \\ &e_g(e_g) : \left.\begin{matrix} \sqrt{(1/3)}d_2 + \sqrt{(2/3)}d_{-1} \\ \sqrt{(1/3)}d_{-2} - \sqrt{(2/3)}d_1 \end{matrix}\right\} : e_g[O_h] \end{aligned} \qquad (A1)$$

where $\Psi = d_m = R(r)/rY_2^m(\theta,\varphi)$, and $R(r)$ and $Y_2^m = \Theta_2^m(\cos\theta)\Phi_m(\varphi)$ are the radial parts of the $3d$ orbitals and the spherical harmonics respectively. The orbital correlation between the C_{3i} and O environments is given in equation ($A1$). The $e_g(e_g)$ orbitals have their maxima along the metal–ligand bonds and have σ character, with a higher orbital energy than the a_g and $e_g(t_{2g})$ orbitals, which have π character and avoid the ligands. The a_g orbital has a maximum along **z**. The form factor:

$$f_{jk} = \int \Psi_j^* \exp(i\mathbf{kr})\,\Psi_k\,d\tau, \quad |\mathbf{k}| = 4\pi\sin\theta/\lambda = k,$$

can be obtained as

$$f_{jk} = \sum_{n=0}^{\infty}\sum_{m=-n}^{n} i^n\langle j_n\rangle_{jk}\,\Theta_n^m(\cos\beta) \times \exp(im\gamma)\sqrt{2(2n+1)}\,C^n(l_jm_j, l_km_k) \qquad (A2)$$

by using the expansion

$$\exp(i\mathbf{kr}) = 4\pi\sum_{n=0}^{\infty}\sum_{m=-n}^{n} i^n j_n(kr)\Theta_n^m(\cos\theta) \times \Phi_m^*(\varphi)\,\Theta_n^m(\cos\beta)\,\Phi_m(\gamma),$$

where the relations,

$$\int_0^{2\pi} \Phi_{m(j)}^*(\varphi)\,\Phi_{m(k)}(\varphi)\,\Phi_m^*(\varphi)\,d\varphi = 1/\sqrt{2\pi},$$

$$\int_0^{\pi} \Theta_{l(j)}^{m(j)*}(\cos\theta)\,\Theta_{l(k)}^{m(k)}(\cos\theta)\,\Theta_n^{m*}(\cos\theta)\sin\theta\,d\theta = \sqrt{(2n+1)/2}\;C^n(l_jm_j, l_km_k),$$

$$\int_0^{\pi} R_j^*(r)\,R_k(r)\,j_n(kr)\,dr = \langle j_n\rangle_{jk}, \quad \text{and} \quad m = m_k - m_j,$$

are used, and $j_n(kr)$ is the nth Bessel function and θ,φ and β,γ are the angular coordinates of **r** and **k** respectively.

The values of $C^n(l_jm_j, l_km_k)$ are tabulated by Condon & Shortley (1935). Since we are concerned with $3d$ electrons, $l_j = l_k = 2$. By using equations ($A1$) and ($A2$), the following expressions can be obtained:

$$f(a_g) = f_{0,0} = \langle j_0\rangle + 5/7(1 - 3\cos^2\beta)\langle j_2\rangle + 9/28(35\cos^4\beta - 30\cos^2\beta + 3)\langle j_4\rangle, \qquad (A3)$$

$$f[e_g(t_{2g})] = \langle j_0\rangle - 5/14(1 - 3\cos^2\beta)\langle j_2\rangle - 1/28(35\cos^4\beta - 30\cos^2\beta + 3)\langle j_4\rangle + 5/\sqrt{2}\cos\beta\sin^3\beta\sin 3\gamma\langle j_4\rangle, \quad (A4)$$

$$f[e_g(e_g)] = \langle j_0\rangle - 1/8(35\cos^4\beta - 30\cos^2\beta + 3)\langle j_4\rangle - 5/\sqrt{2}\cos\beta\sin^3\beta\sin 3\gamma\langle j_4\rangle. \quad (A5)$$

In the aspherical population analysis, $\Delta F[= F_{obs.} - F$ (light atoms) $- F$ (metal cores)] is fitted as $\Delta F = \Sigma n_j f_j$, for $j = a_g$, $e_g(t_{2g})$ and $e_g(e_g)$, where n_j is to be determined by the least-squares method and can be called the electron population parameter (occupation number) of the orbital j.

As can be easily seen, the average form factor, $\bar{f} = 1/5\{f(a_g) + 2f[e_g(t_{2g})] + 2f[e_g(e_g)]\} = \langle j_0\rangle$, is spherically symmetric. The smooth curve of the average factor $\bar{f}$, and the aspherical form factors for each orbital for some arbitrarily chosen reflexions, are shown in Fig. 5 for Cr 3d electrons (80 K), to illustrate the extent of the asphericity.

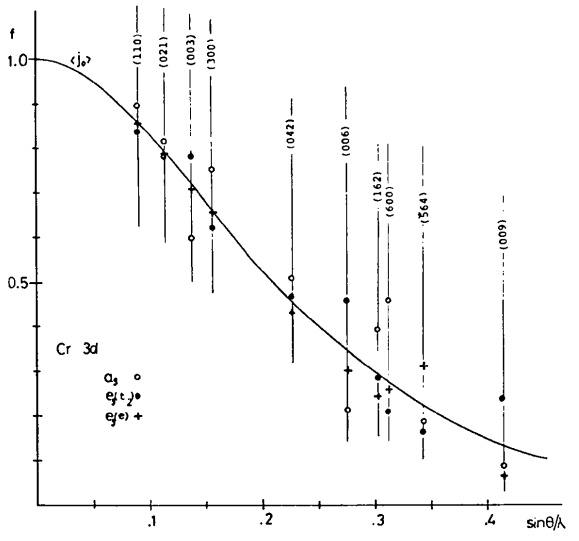

Fig. 5. The atomic form factor for Cr^0 3d at 80 K. Smooth curve: the average spherical factor; O: a_g factor; ●: $e_g(t_{2g})$ factor; +: $e_g(e_g)$ factor, obtained from equations (A3)–(A5).

References

BLESSING, R. H., COPPENS, P. & BECKER, P. (1974). *J. Appl. Cryst.* **7**, 488–492.

CONDON, E. U. & SHORTLEY, G. H. (1935). *Theory of Atomic Spectra*, p. 178. Cambridge Univ. Press.

COPPENS, P. (1975). *Measurement of Electron Densities in Solids by X-ray Diffraction. MTP International Review of Science.* London: Butterworth.

COPPENS, P. & HAMILTON, W. C. (1970). *Acta Cryst.* A**26**, 71–83.

COPPENS, P., LEISEROWITZ, L. & RABINOVICH, D. (1965). *Acta Cryst.* **18**, 1035–1038.

COPPENS, P., PAUTLER, D. & GRIFFIN, J. F. (1971). *J. Amer. Chem. Soc.* **93**, 1051–1058.

COPPENS, P., ROSS, F. K., BLESSING, R. H., COOPER, W. F., LARSEN, F. K., LEIPOLDT, J. G., REES, B. & LEONARD, R. (1974). *J. Appl. Cryst.* **7**, 315–319.

CRUICKSHANK, D. W. J. (1956*a*). *Acta Cryst.* **9**, 757–758.

CRUICKSHANK, D. W. J. (1956*b*). *Acta Cryst.* **9**, 754–756.

CRUICKSHANK, D. W. J. & ROLLETT, J. S. (1953). *Acta Cryst.* **6**, 705–707.

FUKAMACHI, T. (1971). Tech. Rep. B12 of the Inst. of Solid State Physics, Univ. Tokyo.

GRIFFIN, J. F. & COPPENS, P. (1975). *J. Amer. Chem. Soc.* **97**, 3496–3505.

International Tables for X-ray Crystallography (1962). Vol. III. Birmingham: Kynoch Press.

International Tables for X-ray Crystallography (1974). Vol. IV. Birmingham: Kynoch Press.

IWATA, M. & SAITO, Y. (1973). *Acta Cryst.* B**29**, 822–832.

JØRGENSEN, C. K. (1962). *Absorption Spectra and Chemical Bonding in Complexes*, p. 110. New York: Pergamon Press.

MANOHAR, H. & SHWARZENBACH, D. (1974). *Helv. Chim. Acta*, **57**, 1086–1095.

MARUMO, F. & ISOBE, M. (1974). Abstracts, 24th Symposium on Coordination Chemistry, Kanazawa, Japan, p. 95.

MARUMO, F., ISOBE, M. & AKIMOTO, S. (1975). Abstracts, 32nd Annual Meeting of Chem. Soc. Japan, Tokyo, p. 553.

MARUMO, F., ISOBE, M., SAITO, Y., YAGI, T. & AKIMOTO, S. (1974). *Acta Cryst.* B**30**, 1904–1906.

MARUMO, F. & SAITO, Y. (1974). Abstracts, International Crystallography Conference, Melbourne, p. 39.

MASLEN, E. N., RIDOUT, S. C. & WHITE, A. H. (1975). *Acta Cryst.* A**31**, S225.

SHINTANI, H., SATO, S. & SAITO, Y. (1975). *Acta Cryst.* B**31**, 1981–1982.